A Fast Full-Wave Analysis of Scattering and Radiation from Large Finite Arrays of Microstrip Antennas

Chao-Fu Wang, *Member, IEEE*, Feng Ling, *Student Member, IEEE*, and Jian-Ming Jin, *Senior Member, IEEE*

***Abstract*—A fast full-wave analysis technique that can be used to analyze the scattering and radiation from large finite arrays of microstrip antennas is presented. The technique discretizes the mixed potential integral equation (MPIE) in the spatial domain by means of a full-wave discrete complex image method. The del operators on the Green's functions are transferred from the singular kernel to the expansion and testing functions. The resultant system of equations is solved using the biconjugate gradient (BCG) method in which the matrix–vector product is evaluated efficiently using fast Fourier transform (FFT). This results in an efficient and accurate computation of the scattering and radiation from finite arrays of microstrip antennas. Several numerical results are presented, demonstrating the accuracy, efficiency, and capability of this technique.**

***Index Terms*—Microstrip arrays, numerical method.**

I. Introduction

MICROSTRIP antennas and arrays have several unique features, which make them attractive candidates for many antenna applications, ranging from mobile communications to phased-array radar systems. A microstrip antenna array can be analyzed using two approaches. One approach is to approximate the array as an infinite array and, as a result, the analysis of the array is then reduced to the analysis of a single element using Floquet-type representation of fields [1]–[3]. This approach is very efficient; however, it does not account for the edge effects of a finite array nor can it deal with the effect of the feed network. The other approach is to deal with the finite array directly. This approach is considerably more difficult because of the necessity of solving a large matrix equation, which requires a large computer memory and excessive computing time. In the past, finite arrays of printed dipoles and rectangular microstrip patches have been studied by using the spectral-domain moment methods [4]–[6]. A microstrip series-fed array has also been analyzed [7] using a full-wave discrete image technique that transforms a spectral-domain formulation into the spatial domain without losing any full-wave information [8], [9].

A powerful numerical technique that can significantly reduce the memory requirement and computing time is to combine the conjugate gradient (CG) method with the fast Fourier transform (FFT). The resultant method is often referred to as the CG-FFT method. This method was first developed by Bojarski [10] and has been applied to many large electromagnetic problems. The CG-FFT method can be implemented in several different schemes, which differ primarily in the manner in which the derivatives are treated and the Green's functions are calculated. A comparison of some of these methods as applied to the flat-plate scattering problem can be found in [11] and [12]. The results indicate two important facts. First, the conventional CG-FFT method [11], [13] usually requires a large FFT pad to reduce aliasing errors since the analytical Fourier transform of the Green's function extends over the entire space. This problem can be overcome by using a spatial discretization scheme [12], [14]. Second, a much more accurate and efficient solution can be achieved by transferring the del operators from the Green's function to the expansion and testing functions [12]. Realizing these two facts, a full-wave analysis technique for microstrip structures has been proposed, which combines the CG-FFT method with the full-wave discrete image technique [15].

When a spatial-domain discretization is used in the CG-FFT method, the efficiency of the method is primarily determined by the convergence of the CG algorithm. In many applications, the CG algorithm can be substituted by other iterative algorithms for a faster convergence. A commonly used alternative is the biconjugate gradient (BCG) algorithm. The BCG algorithm for solving linear systems was first developed by Lanczos [16] and discussed by Fletcher [17] and Jacobs [18]. This algorithm has several significant features that make it an attractive alternative to the standard CG algorithm. For example, the BCG algorithm requires only one matrix–vector product per iteration for solving symmetric systems. Furthermore, it does not square the condition number, which generally translates to an improved convergence rate [19], although it does not decrease the residual error monotonically. Therefore, the BCG algorithm is better suited for systems that are poorly conditioned than the CG algorithm. It is found that in the application dealt with in this paper, the BCG algorithm outperforms the CG algorithm significantly.

Manuscript received August 4, 1997; revised June 2, 1998. This work was supported in part by the Office of Naval Research under Grant N00014-95-1-0848, the National Science Foundation under Grant NSF ECE 94-57735, and a Grant from AFOSR via the MURI Program under Contract F49620-96-1-0025.

The authors are with the Electromagnetics Laboratory and Center for Computational Electromagnetics, Department of Electrical and Computer Engineering, University of Illinois at Urbana-Champaign, Urbana, IL 61801 USA.

Publisher Item Identifier S 0018-926X(98)07531-0.

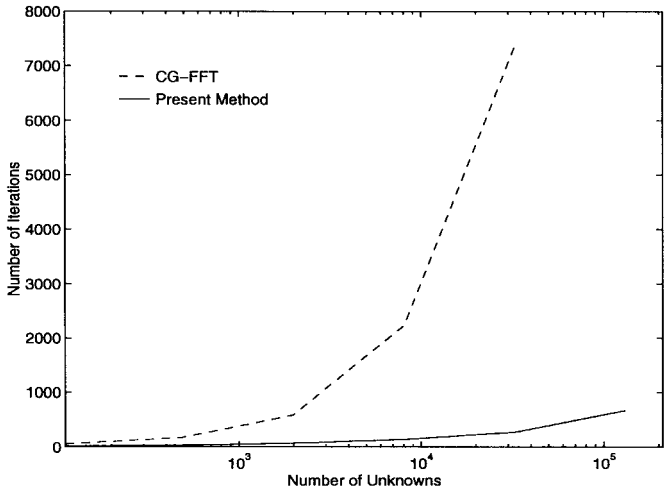

Fig. 1. The number of iterations versus the number of unknowns.

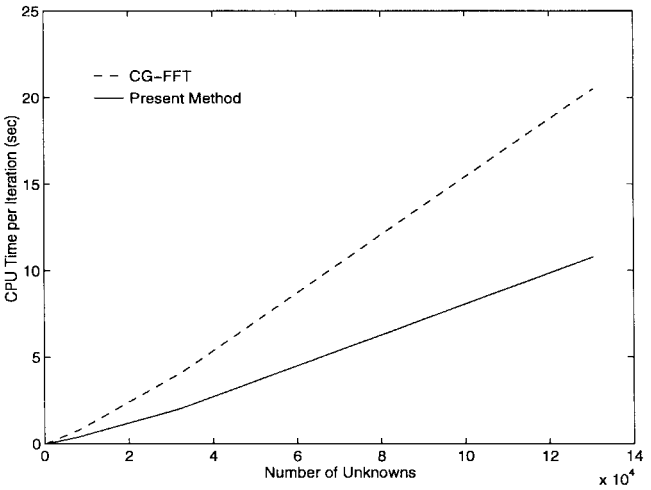

Fig. 2. The CPU time per iteration versus the number of unknowns.

In this paper, we present a new fast full-wave analysis technique that can be used to analyze large microstrip antenna arrays. We discretize the integral equation describing the microstrip problem by converting the spectral domain Green's functions into the closed-form spatial Green's functions by means of full-wave discrete image representations. In this procedure, the del operators are transferred from the singular kernel to the expansion and testing functions. The BCG algorithm in conjunction with the FFT is then employed to solve the resulting system of equations. Once the currents on the microstrip antennas are obtained, the radar cross section (RCS) and radiation pattern are calculated using the reciprocity theorem. The numerical results show that the proposed method is efficient for the analysis of large microstrip antenna arrays.

II. MPIE and Discretization

To set up an integral equation that can be used to solve the problem of scattering and radiation from a microstrip patch antenna, we start with the boundary condition associated with the tangential electric field on a perfectly conducting surface

$$\hat{n} \times \mathbf{E}^s(\mathbf{r}) = -\hat{n} \times [\mathbf{E}^i(\mathbf{r}) + \mathbf{E}^r(\mathbf{r})] \text{ on } S \tag{1}$$

where S denotes the conducting surface of the antenna, $\mathbf{E}^s$ denotes the scattered field excited by the current on S, $\mathbf{E}^i$ denotes the incident electric field given by

$$\mathbf{E}^i(\mathbf{r}) = (\hat{\theta}^i E_\theta + \hat{\phi}^i E_\phi) e^{-j\mathbf{k}^i \cdot \mathbf{r}} \tag{2}$$

for a plane-wave incidence, and $\mathbf{E}^r$ denotes the reflected field by the grounded dielectric substrate in the absence of the antenna, which can be written as

$$\mathbf{E}^r(\mathbf{r}) = (\hat{\theta}^r R^{\mathrm{TM}} E_\theta + \hat{\phi}^r R^{\mathrm{TE}} E_\phi) e^{-j\mathbf{k}^r \cdot \mathbf{r}} \tag{3}$$

where R^{TM} and R^{TE} are the reflection coefficients at the interface of the air and dielectric substrate for the TM and TE incidences, respectively.

For microstrip structures, the mixed potential integral equation (MPIE) yields a weaker singularity in its integrands than the electric field integral equation (EFIE). The MPIE for (1) can be written as

$$j\omega\mu_0 \hat{n} \times \left[\mathbf{A}(\mathbf{r}) + \frac{1}{k_0^2} \nabla \Phi(\mathbf{r})\right] = \hat{n} \times [\mathbf{E}^i(\mathbf{r}) + \mathbf{E}^r(\mathbf{r})] \tag{4}$$

where

$$\mathbf{A}(\mathbf{r}) = \iint_S \overline{\mathbf{G}}_A(\mathbf{r}, \mathbf{r}') \cdot \mathbf{J}(\mathbf{r}')\, ds' \tag{5}$$

$$\Phi(\mathbf{r}) = \iint_S G_q(\mathbf{r}, \mathbf{r}') \nabla \cdot \mathbf{J}(\mathbf{r}')\, ds' \tag{6}$$

in which $\mathbf{J}$ is the unknown current on the microstrip antenna, $\overline{\mathbf{G}}_A$, and G_q denote the Green's functions for the magnetic vector potential and the electric scalar potential, respectively.

The spatial-domain Green's functions $\overline{\mathbf{G}}_A$ and G_q are the key to the discretization of the MPIE in the spatial domain. The $\overline{\mathbf{G}}_A$ has four components; however, only the xx and yy components are used in the solution of (4) for the unknown current $\mathbf{J}$. These two components are denoted here as G_a. The Green's functions G_a and G_q can be written in the form of the Sommerfeld integral

$$G_{a,q}(\rho) = \int_{-\infty}^{+\infty} \tilde{G}_{a,q}(k_\rho) H_0^{(2)}(k_\rho \rho) k_\rho\, dk_\rho \tag{7}$$

where $\tilde{G}_{a,q}$ denote the spectral domain Green's functions. Generally, this inverse Hankel transform cannot be solved analytically. Fortunately, a full-wave discrete complex image technique has been developed for a rapid evaluation of this integral [8], [9], yielding closed-form spatial Green's functions.

As illustrated in [8] and [9], the discrete complex image method extracts the quasi-dynamic and surface wave contributions from the spectral-domain Green's function and approximates the remainder as complex images by Prony's method. The spatial-domain Green's function can then be obtained analytically using the Sommerfeld identity. When this is applied to (7), one obtains

$$G_{a,q} = G_{a,q}^{(qd)} + G_{a,q}^{(sw)} + G_{a,q}^{(ci)} \tag{8}$$

where $G^{(qd)}$ represents the contribution from the quasi-dynamic (qd) images, which dominates in the near-field

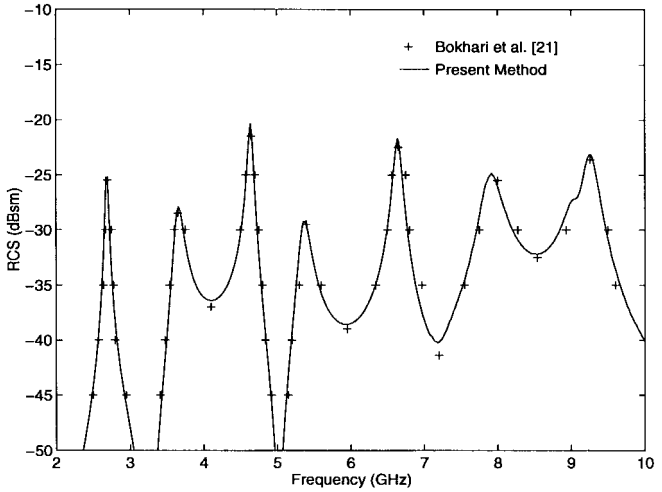

Fig. 3. The RCS ($\sigma_{\theta\theta}$) versus frequency for a rectangular microstrip patch antenna (patch size: 36.6 mm × 26.0 mm, $\varepsilon_r = 2.17$, substrate thickness: $h = 1.58$ mm, $\theta^i = 60°$, $\phi^i = 45°$).

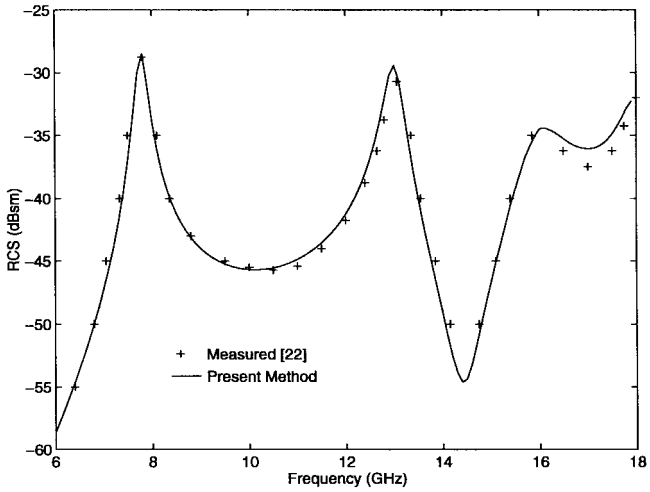

Fig. 4. The RCS ($\sigma_{\theta\theta}$) versus frequency for a circular microstrip patch antenna (patch radius: $r = 7.1$ mm, $\varepsilon_r = 2.2$, substrate thickness: $h = 0.7874$ mm, $\theta^i = 63°$, $\phi^i = 0°$).

region, $G^{(sw)}$ represents the contribution from the surface waves (sw), which dominates in the far-field region, and $G^{(ci)}$ represents the contribution from the complex images (ci), which dominates in the intermediate region. The specific forms of G_a and G_q can be written as

$$G_a = G_a^{(qd)} + G_a^{(sw)} + G_a^{(ci)} \tag{9}$$

where

$$G_a^{(qd)} = \frac{e^{-jk_0 r_0}}{4\pi r_0} - \frac{e^{-jk_0 r_1}}{4\pi r_1} \tag{10}$$

$$G_a^{(sw)} = \frac{1}{2j} \sum_{p(\mathrm{TE})} R_a H_0^{(2)}(k_{\rho p}\rho) k_{\rho p} \tag{11}$$

$$G_a^{(ci)} = \sum_{i=1}^{N} a_i \frac{e^{-jk_0 r_i'}}{4\pi r_i'} \tag{12}$$

and

$$G_q = G_q^{(qd)} + G_q^{(sw)} + G_q^{(ci)} \tag{13}$$

where

$$G_q^{(qd)} = (1+K)\frac{e^{-jk_0 r_0}}{4\pi r_0} + (K^2-1)\frac{e^{-jk_0 r_1}}{4\pi r_1} - K\frac{e^{-jk_0 r_2}}{4\pi r_2} - K^2\frac{e^{-jk_0 r_3}}{4\pi r_3} \tag{14}$$

$$G_q^{(sw)} = \frac{1}{2j} \sum_{p(\mathrm{TE,\,TM})} R_q H_0^{(2)}(k_{\rho p}\rho) k_{\rho p} \tag{15}$$

$$G_q^{(ci)} = \sum_{i=1}^{N} a_i' \frac{e^{-jk_0 r_i''}}{4\pi r_i''}. \tag{16}$$

In the above, $r_n = \sqrt{\rho^2 + (2nh)^2}$ with h being the thickness of the substrate, $r_i' = \sqrt{\rho^2 - b_i^2}$ and $r_i'' = \sqrt{\rho^2 - b_i'^2}$ where b_i and b_i' are complex numbers determined together with a_i and a_i' by Prony's method, and $K = (1-\epsilon_r)/(1+\epsilon_r)$ with ϵ_r being the relative permittivity of the substrate. Furthermore, $k_{\rho p}$ is the surface wave pole located on the real axis of the complex k_ρ plane and R_a and R_q are the residues of the integrand at the pole $k_\rho = k_{\rho p}$. The summation in (11) carries over the poles of the TE surface waves and the summation in (15) carries over the poles of both the TE and TM surface waves. The N in (12) and (16) denotes the number of complex images and usually $N = 3$ for an accuracy with less than 1% error.

With the intent of computing the left-hand side of (4) via the FFT, we place the conducting surface of the antenna in a rectangular area which is then divided into $M \times N$ small rectangular cells whose side lengths are Δx and Δy along the x and y directions, respectively. Assume that $\mathbf{f}_{m,n}^x = f_{m,n}^x \hat{x}$ and $\mathbf{f}_{m,n}^y = f_{m,n}^y \hat{y}$ are vector basis functions in the x and y directions, respectively, where $f_{m,n}^{x,y}$ represent the roof-top functions. The Galerkin's formulation for solving (4) can be written as

$$j\omega\mu_0 \langle \mathbf{f}_{m,n}^{x,y}, \mathbf{A} \rangle - \frac{1}{j\omega\epsilon_0} \langle \Phi, \nabla \cdot \mathbf{f}_{m,n}^{x,y} \rangle = \langle \mathbf{f}_{m,n}^{x,y}, \mathbf{E}^i(\mathbf{r}) + \mathbf{E}^r(\mathbf{r}) \rangle \tag{17}$$

where $\langle \cdot \rangle$ denotes the inner product of two vector functions. We can expand the surface-current distribution $\mathbf{J}$ in a sequence of vector basis functions $\mathbf{f}_{m,n}^x$ and $\mathbf{f}_{m,n}^y$ as follows:

$$\mathbf{J} = \sum_{m,n} I_{m,n}^x \mathbf{f}_{m,n}^x + \sum_{m,n} I_{m,n}^y \mathbf{f}_{m,n}^y. \tag{18}$$

Substituting (18) into (17), we obtain the following:

$$\begin{bmatrix} \mathbf{G}_{xx} & \mathbf{G}_{xy} \\ \mathbf{G}_{yx} & \mathbf{G}_{yy} \end{bmatrix} \begin{bmatrix} \mathbf{J}_x \\ \mathbf{J}_y \end{bmatrix} = \begin{bmatrix} \mathbf{b}_x \\ \mathbf{b}_y \end{bmatrix} \tag{19}$$

where

$$\begin{aligned} \mathbf{G}_{xx} &= [G_{xx}(m-m', n-n')] \\ \mathbf{G}_{xy} &= [G_{xy}(m-m', n-n')] \\ \mathbf{G}_{yx} &= [G_{yx}(m-m', n-n')] \\ \mathbf{G}_{yy} &= [G_{yy}(m-m', n-n')] \\ \mathbf{b}_x &= [\langle \mathbf{f}_{m,n}^x, \mathbf{E}^i(\mathbf{r}) + \mathbf{E}^r(\mathbf{r}) \rangle] \\ \mathbf{b}_y &= [\langle \mathbf{f}_{m,n}^y, \mathbf{E}^i(\mathbf{r}) + \mathbf{E}^r(\mathbf{r}) \rangle] \end{aligned}$$

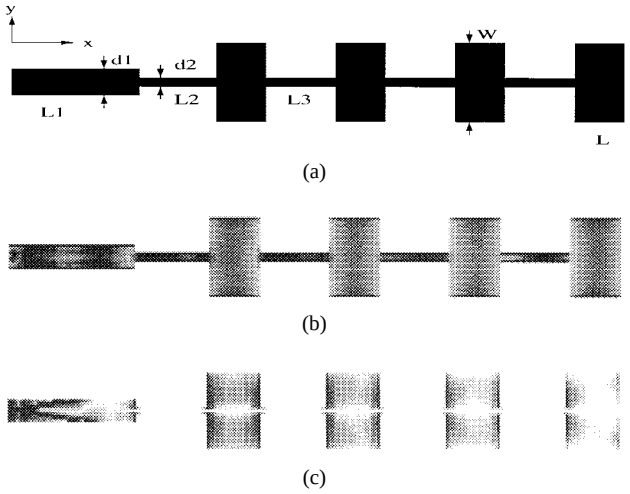

Fig. 5. The current on a series-fed microstrip antenna array $L = 10.08$ mm, $W = 11.79$ mm, $L_1 = 23.6$ mm, $L_2 = 13.4$ mm, $L_3 = 12.32$ mm, $d_1 = 3.93$ mm, $d_2 = 1.3$ mm, the thickness of substrate $h = 1.5748$ mm, $\epsilon_r = 2.1$, $f = 9.42$ GHz. (a) Geometry. (b) x-directed current. (c) y-directed current.

in which

$$G_{xx}(m-m', n-n') = \Gamma_a^x(m-m', n-n') + \Gamma_{xx}(m-m', n-n')$$

$$G_{xy}(m-m', n-n') = \frac{1}{\Delta x \Delta y}\sum_{i=0}^{1}\sum_{k=0}^{-1}(-1)^{i+k}\Gamma_q(m-m'+i, n-n'+k)$$

$$G_{yy}(m-m', n-n') = \Gamma_a^y(m-m', n-n') + \Gamma_{yy}(m-m', n-n')$$

$$G_{yx}(m-m', n-n') = G_{xy}(n'-n, m'-m)$$

and

$$\Gamma_{xx}(m-m', n-n') = \frac{1}{(\Delta x)^2}\sum_{i=0}^{1}\sum_{k=0}^{-1}(-1)^{i+k}\Gamma_q(m-m'+i+k, n-n')$$

$$\Gamma_{yy}(m-m', n-n') = \frac{1}{(\Delta y)^2}\sum_{i=0}^{1}\sum_{k=0}^{-1}(-1)^{i+k}\Gamma_q(m-m', n-n'+i+k)$$

$$\Gamma_a^x(m-m', n-n') = j\omega\mu_0 \iint_S f_{m,n}^x \iint_S G_a f_{m',n'}^x \, ds' ds$$

$$\Gamma_a^y(m-m', n-n') = j\omega\mu_0 \iint_S f_{m,n}^y \iint_S G_a f_{m',n'}^y \, ds' ds,$$

$$\Gamma_q(m-m', n-n') = \frac{j}{\omega\varepsilon_0} \iint_S \Pi_{m,n} \iint_S G_q \Pi_{m',n'} \, ds' ds.$$

In the above, $\Pi_{m,n}$ is the two-dimensional (2-D) unit pulse function defined over (m, n)th rectangular cell.

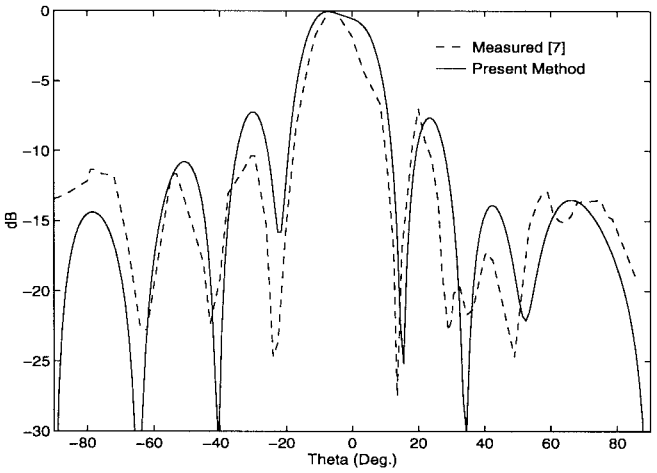

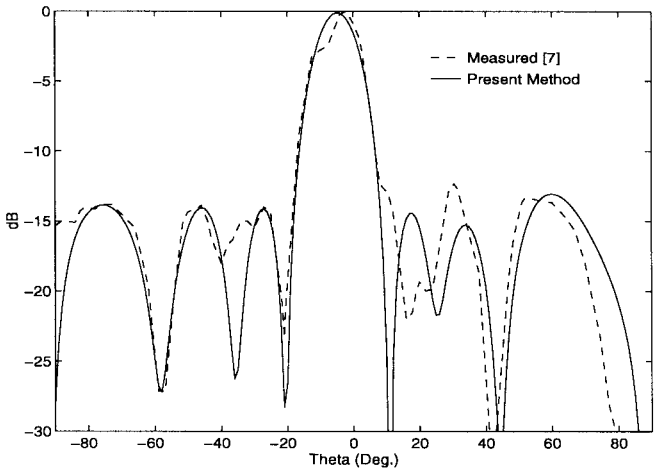

Fig. 6. The E-plane radiation patterns of a series-fed microstrip antenna array. (a) $L_1 = 23.6$ mm. (b) $L_1 = 14.6$ mm.

III. BCG-FFT Solution

The linear system implied by (19) can be solved via either a direct or an iterative method. In order to analyze large finite arrays of microstrip antennas, we employ the BCG algorithm and FFT to significantly reduce the memory requirement and central processing unit (CPU) time. The BCG algorithm employed here for the solution of $Ax = b$ in which A is symmetric can be found in [12] and [19]. In this BCG algorithm, A is only involved in the matrix–vector product. For the problem considered here this product can be computed efficiently via FFT without a need to generate the square matrix.

In fact, it is observed that the relationship between $\overline{\mathbf{G}}_A$ and $\mathbf{J}$ is a convolution. Therefore, we can obtain the following discrete convolution relationship:

$$\mathbf{G}_{xx}\mathbf{J}_x = DFT^{-1}\{DFT\{G_{xx}(m, n)\} \cdot DFT\{J_x(m, n)\}\} \quad (20)$$

$$\mathbf{G}_{yy}\mathbf{J}_y = DFT^{-1}\{DFT\{G_{yy}(m, n)\} \cdot DFT\{J_y(m, n)\}\}. \quad (21)$$

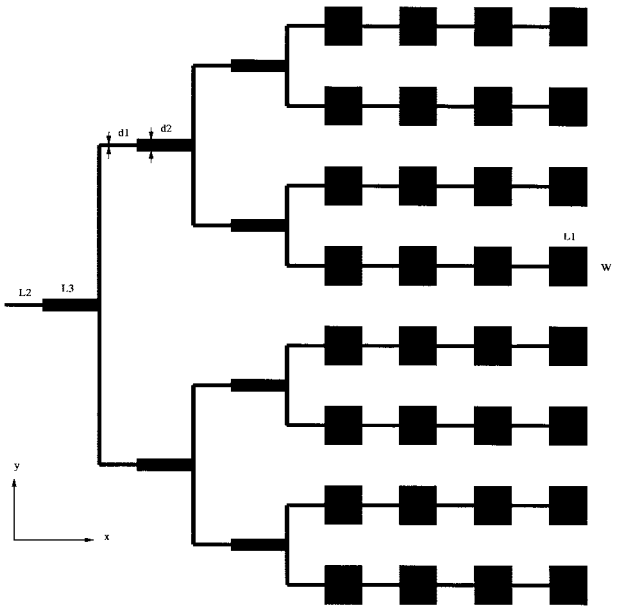

Fig. 7. The geometry of 8×4 microstrip corporate-fed planar array, $L_1 = 10.08$ mm, $L_2 = 12.32$ mm, $L_3 = 18.48$ mm, $W = 11.79$ mm, $d_1 = 1.3$ mm, $d_2 = 3.93$ mm, the thickness of substrate $h = 1.59$ mm, $\epsilon_r = 2.2$, $f = 9.42$ GHz.

It is also observed that the relationship between G_q and $\nabla \cdot \mathbf{J}$ is a convolution. Thus, the following discrete convolution relationship can be obtained:

$$\mathbf{G}_{xy}\mathbf{J}_y = [D_y(m, n) - D_y(m+1, n)] \tag{22}$$

$$\mathbf{G}_{yx}\mathbf{J}_x = [D_x(m, n) - D_x(m, n+1)] \tag{23}$$

where

$$[D_x(m, n)] = \frac{1}{\Delta x \Delta y} DFT^{-1}\{\Gamma_{qx}(m, n)\} \tag{24}$$

$$[D_y(m, n)] = \frac{1}{\Delta x \Delta y} DFT^{-1}\{\Gamma_{qy}(m, n)\} \tag{25}$$

and

$$[\Gamma_{qx}(m, n)] = DFT\{\Gamma_q(m, n)\} \cdot DFT\{J_x(m, n) - J_x(m-1, n)\} \tag{26}$$

$$[\Gamma_{qy}(m, n)] = DFT\{\Gamma_q(m, n)\} \cdot DFT\{J_y(m, n) - J_y(m, n-1)\}. \tag{27}$$

Apparently, the matrix–vector product can be calculated efficiently via FFT by using (20)–(27).

IV. Far-Field Calculation

Once the surface currents are obtained, the scattered or radiated field in the far-field zone can be evaluated conveniently using the reciprocity theorem [20]. In accordance with the reciprocity theorem, the field ($\mathbf{E}^{sc,\,rad}$) radiated by $\mathbf{J}$ in the presence of the grounded dielectric substrate is related to $\mathbf{J}$ by

$$\iiint \mathbf{E}^{sc,\,rad} \cdot \mathbf{J}_2 \, dv = \iint_S \mathbf{E}_2 \cdot \mathbf{J} \, ds \tag{28}$$

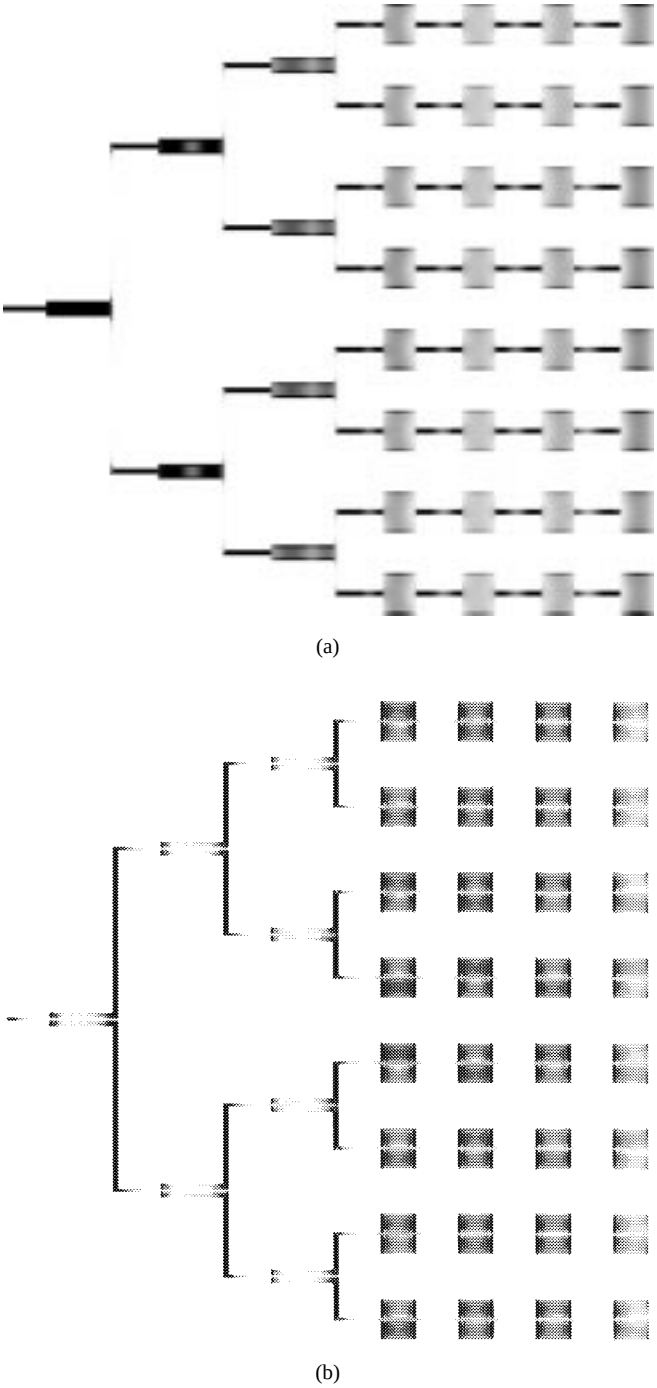

(a)

(b)

Fig. 8. The current distribution on the 8×4 microstrip corporate-fed planar array. (a) The x-directed current. (b) The y-directed current.

where $\mathbf{J}_2$ denotes an arbitrary electric current and $\mathbf{E}_2$ is the field radiated by $\mathbf{J}_2$ in the presence of the grounded dielectric substrate. Choosing an infinitesimal electric current element, either θ-polarized or ϕ-polarized, and placing it at the observation point in the far zone, we can compute the electric field ($\mathbf{E}_{\theta,\,\phi}$) in the presence of the dielectric substrate without the patch antenna, where $\mathbf{E}_\theta$ is due to the θ-polarized electric current element and $\mathbf{E}_\phi$ due to the ϕ-polarized electric current element. In the backscatter case, they are the same as those in the right-hand side of (1). Hence, from the reciprocity theorem,

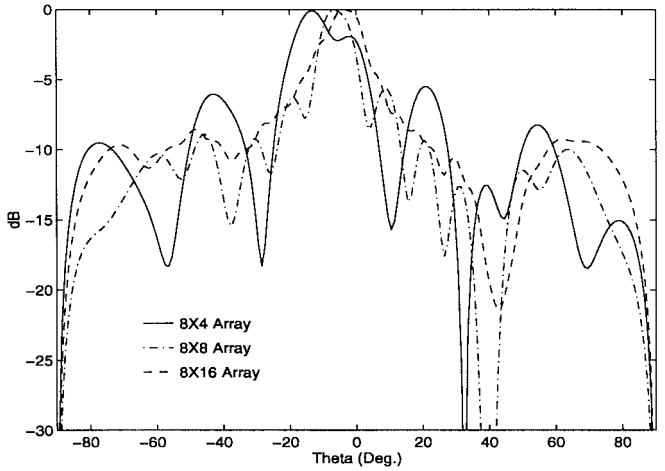

(a)

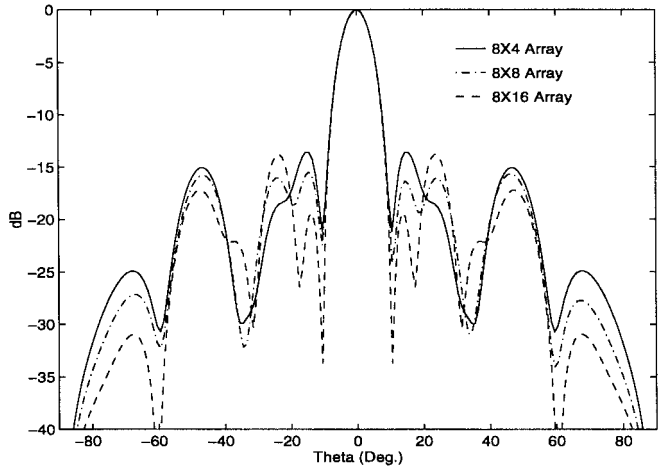

(b)

Fig. 9. The radiation patterns of the $8 \times N$ microstrip corporate-fed planar array. (a) E-plane pattern. (b) H-plane pattern.

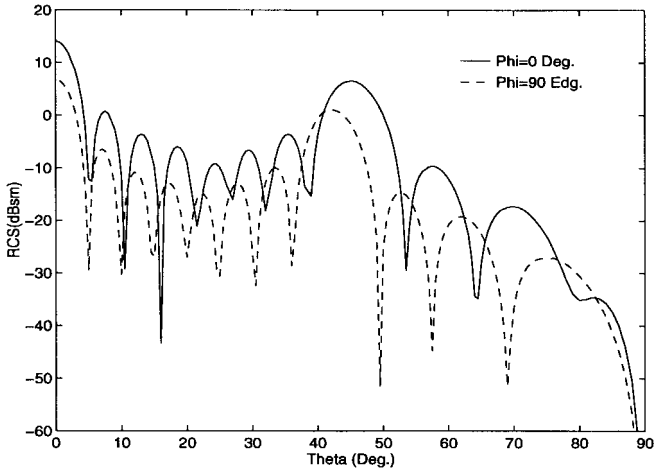

(a)

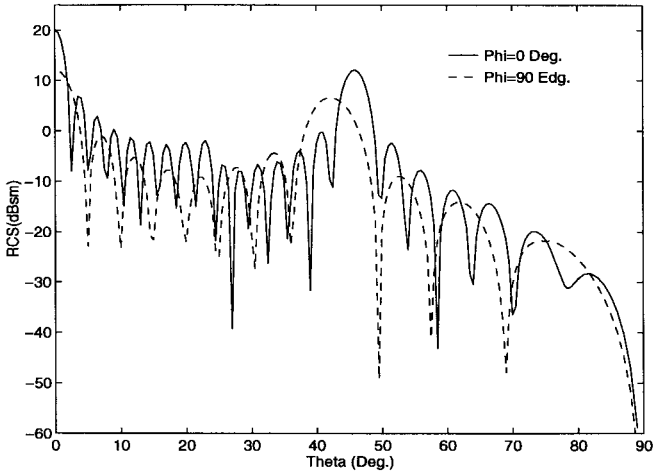

(b)

Fig. 10. The monostatic RCS of the microstrip corporate fed planar arrays. (a) 8×8 array. (b) 8×16 array.

we can obtain the scattered/radiated field as

$$E_{\theta,\phi}^{sc,rad}(\mathbf{r}) = -\frac{j\omega\mu_0 e^{-jk_0 r}}{4\pi r} \iint_S \mathbf{J}(\mathbf{r}) \cdot \mathbf{E}_{\theta,\phi}\, ds. \quad (29)$$

In the case of scattering, if the incident field is polarized in the u direction and the v component of the scattered field is considered, where u and v can be θ or ϕ, then the RCS is given by

$$\sigma_{uv} = \lim_{r\to\infty} 4\pi r^2 \frac{|E_v^{sc}|^2}{|E_u^i|^2}. \quad (30)$$

V. Numerical Results

In this section, we present several numerical results to demonstrate the accuracy and efficiency of the method described above. The normalized residual is defined as $Err = ||\mathbf{r}_n||^2/||\mathbf{b}||^2$. All computations are carried out on a DEC Alpha workstation.

In order to test the convergence of the method, we first consider the problem of scattering by a rectangular microstrip patch antenna at normal incidence [21] (patch size: 10 mm $\times$ 15 mm, $\varepsilon_r = 10.2$, substrate thickness: $h = 1.27$ mm, $f = 3.12$ GHz). For a given tolerance $Err < 10^{-6}$, the number of iterations and the CPU time per iteration versus the number of unknowns for the CG-FFT [15] and for the present method are given in Figs. 1 and 2. Both figures show that the convergence behavior and the efficiency of the present method are much better than that of the CG-FFT method.

As the second test case, we consider the scattering from a rectangular microstrip patch antenna (patch size: 36.6 mm $\times$ 26.0 mm, $\varepsilon_r = 2.17$, substrate thickness: $h = 1.58$ mm, incident angle: $\theta^i = 60°$, $\phi^i = 45°$). The monostatic RCS is given in Fig. 3 as a function of frequency and is compared with the result in [22]. The two results agree very well, demonstrating that the proposed method has a good accuracy.

The third case concerns the scattering from a circular microstrip patch antenna (circular patch radius: $r = 7.1$ mm, $\varepsilon_r = 2.2$, substrate thickness: $h = 0.7874$ mm, incident angle: $\theta^i = 63°$, $\phi^i = 0°$). The monostatic RCS is given in Fig. 4 as a function of frequency and is compared with the measured data [23], showing a good agreement.

As the fourth example, we consider the radiation from a four-element series-fed microstrip antenna array, which is fed at the left end. The geometric parameters and current

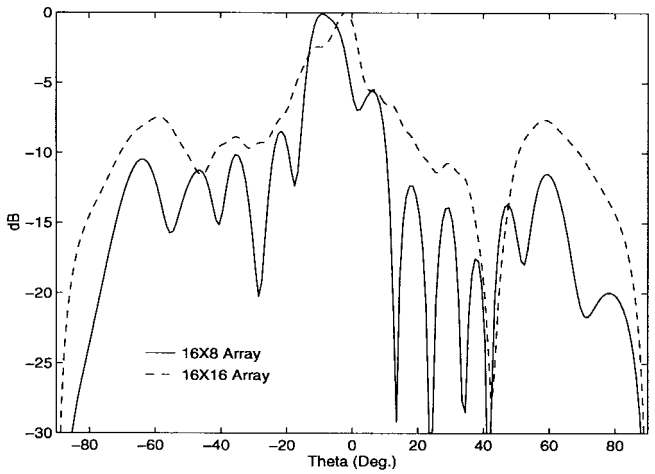

(a)

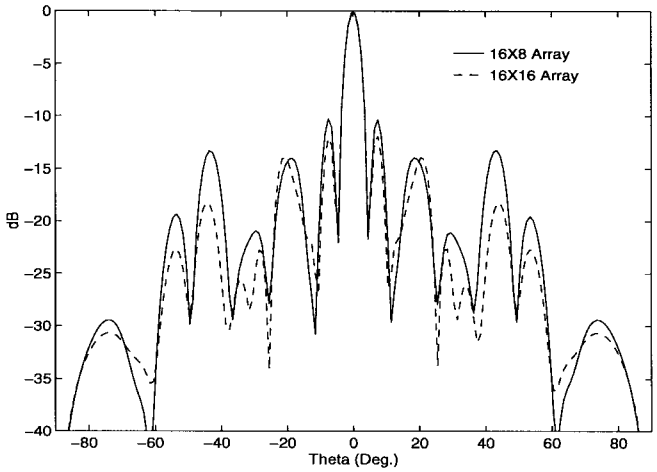

(b)

Fig. 11. The radiation patterns of the 16 × 8 and 16 × 16 microstrip corporate-fed planar arrays. (a) E-plane pattern. (b) H-plane pattern.

distributions are given in Fig. 5. The E-plane radiation pattern is given in Fig. 6 and is compared with the measured data [7].

The last example concerns the scattering and radiation from microstrip corporate fed planar arrays to test the capability of the proposed method. The 8 × 4 microstrip corporate-fed planar array is depicted in Fig. 7, where $\varepsilon_r = 2.2$ and the substrate thickness is $h = 1.59$ mm. The current distributions on the 8 × 4 microstrip corporate-fed planar array are given in Fig. 8 and the radiation patterns are given in Fig. 9. In calculating the radiation patterns, we have increased the number of microstrip patch elements in each arm from 4 to 16 to show the effect on the radiation pattern. The monostatic RCS of the same structure are given in Fig. 10. Finally, the radiation patterns of a 16 × 8 and a 16 × 16 microstrip corporate-fed planar array are given in Fig. 11. The requirement of computational resources is listed in Table I.

VI. Conclusion

A fast full-wave analysis method for simulating the scattering and radiation from large finite arrays of microstrip antennas is presented. In this method, the MPIE is discretized in the spatial domain by means of a full-wave discrete image technique. This keeps the necessary FFT pad size to the minimum and results in a more efficient code. The resulting system is solved using BCG algorithm in conjunction with FFT. Numerical results show that the proposed method is more efficient than the CG-FFT method and requires minimum memory and CPU time.

TABLE I
CPU Time and Storage of DEC Alpha Workstation

Array	Number of Unknowns	CPU Time per Iteration	Number of Iterations	Computer Storage	Tolerance Err
8 × 8	118 073	11.6 s	313	18 Mb	10^{-3}
8 × 8	118 073	11.6 s	599	18 Mb	10^{-6}
16 × 16	495 044	97.81 s	425	65 Mb	10^{-3}
16 × 16	495 044	97.81 s	1070	65 Mb	10^{-6}

Acknowledgment

The authors would like to thank Prof. D. G. Fang at Nanjing University of Science and Technology, who taught them much about the discrete complex image method.

References

[1] D. M. Pozar and D. H. Schaubert, "Scan blindness in infinite phased arrays of print diploes," *IEEE Trans. Antennas Propagat.*, vol. AP-32, pp. 602–610, June 1984.

[2] ——, "Analysis of an infinite array of rectangular microstrip patches with idealized probe feeds," *IEEE Trans. Antennas Propagat.*, vol. AP-32, pp. 1101–1107, Oct. 1984.

[3] C. C. Liu, J. Shmoys, A. Hesel, J. D. Hanfling, and J. M. Usoff, "Plane wave reflection from microstrip-patch array—Theory and experiment," *IEEE Trans. Antennas Propagat.*, vol. AP-33, pp. 426–435, Apr. 1985.

[4] D. M. Pozar, "Analysis of finite phased arrays of printed dipoles," *IEEE Trans. Antennas Propagat.*, vol. AP-33, pp. 1045–1053, Oct. 1985.

[5] ——, "Finite phased arrays of rectangular microstrip patches," *IEEE Trans. Antennas Propagat.*, vol. AP-34, pp. 658–665, May 1986.

[6] A. S. King and W. J. Bow, "Scattering from a finite array of microstrip patches," *IEEE Trans. Antennas Propagat.*, vol. 40, pp. 770–774, July 1992.

[7] K. L. Wu, M. Spenuk, J. Litva, and D. G. Fang, "Theoretical and experimental study of feed network effects on the radiation pattern of series-fed microstrip antenna arrays," *Proc. Inst. Elect. Eng.*, vol. 138, pt. H, pp. 238–242, June 1991.

[8] D. G. Fang, J. J. Yang, and G. Y. Delisle, "Discrete image theory for horizontal electric dipole in a multilayer medium," *Proc. Inst. Elect. Eng.*, vol. 135, pt. H, pp. 297–303, Oct. 1988.

[9] Y. L. Chow, J. J. Yang, D. G. Fang, and G. E. Howard, "A closed-form spatial Green's function for the thick microstrip substrate," *IEEE Trans. Microwave Theory Tech.*, vol. 39, pp. 588–592, Mar. 1991.

[10] N. N. Bojarski, "k-space formulation of the electromagnetic scattering problem," Air Force Avionics Lab., Tech. Rep. AFAL-TR-71-75, Mar. 1971.

[11] A. P. M. Zwamborn and P. M. van den Berg, "A weak form of the conjugate gradient FFT method for plate problems," *IEEE Trans. Antennas Propagat.*, vol. 39, pp. 224–228, Feb. 1991.

[12] J. M. Jin and J. L. Volakis, "A biconjugate gradient solution for scattering by planar plates," *Electromagn.*, vol. 12, pp. 105–119, 1992.

[13] T. K. Sarkar, E. Arvas, and S. M. Rao, "Application of FFT and the conjugate gradient method for the solution of electromagnetic radiation from electrically large and small conducting bodies," *IEEE Trans. Antennas Propagat.*, vol. AP-34, pp. 635–640, May 1986.

[14] M. F. Catedra, J. G. Cuevas, and L. Nuno, "A scheme to analyze conducting plates of resonant size using the conjugate gradient method

and fast Fourier transform," *IEEE Trans. Antennas Propagat.*, vol. 36, pp. 1744–1752, Dec. 1988.

[15] Y. Zhuang, K. L. Wu, C. Wu, and J. Litva "A combined full-wave CG-FFT method for rigorous analysis of large microstrip antenna arrays," *IEEE Trans. Antennas Propagat.*, vol. 44, pp. 102–109, Jan. 1996.

[16] C. Lanczos, "An iteration method for the solution of the eigenvalue problem of linear differential and integral operators," *J. Res. Nat. Bur. Stand.*, vol. 45, pp. 255–282, 1950.

[17] R. Fletcher, "Conjugate gradient methods for indefinte systems," in *Numerical Analysis Dundee*, G. A. Watson, Ed. New York: Springer-Verlag, pp. 73–79, 1975/1976.

[18] D. A. H. Jacobs, "The exploitation of sparsity by iterative methods," in *Sparse Matrices and Their Uses*, I. S. Duff, Ed. Berlin, Germany: Springer-Verlag, pp. 191–222, 1981.

[19] C. F. Smith, A. F. Peterson, and R. Mittra, "The biconjugate gradient method for electromagnetic scattering," *IEEE Trans. Antennas Propagat.*, vol. 38, pp. 938–940, June 1990.

[20] N. G. Alexopoulos and D. R. Jackson, "Fundamental superstrate (cover) effects on printed circuit antennas," *IEEE Trans. Antennas Propagat.*, vol. AP-32, pp. 807–816, Aug. 1984.

[21] M. F. Catedra and M. Gago, "Spectral domain analysis of conducting patches of arbitrary geometry in multilayer media using the CG-FFT method," *IEEE Trans. Antennas Propagat.*, vol. 38, pp. 1530–1536, Oct. 1990.

[22] S. A. Bokhari, J. R. Mosig, and F. E. Gardiol, "Radar cross section computation of microstrip patches," *Electromagn.*, vol. 14, pp. 19–32, 1994.

[23] J. T. Aberle, D. M. Pozar, and C. R. Birtcher, "Evaluation of input impedance and radar cross section of probe-fed microstrip patch elements using an accurate feed model," *IEEE Trans. Antennas Propagat.*, vol. 39, pp. 1691–1696, Dec. 1991.

Chao-Fu Wang (M'98) was born on November 15, 1964, in Henan, China. He received the B.Sc. degree in mathematics from Henan Normal University, Xinxiang, China, in 1985, the M.Sc. degree in applied mathematics from Hunan University, Changsha, China, 1989, and the Ph.D. degree in electrical engineering from the University of Electronic Science and Technology of China, Chengdu, China, 1995.

From 1987 to 1996, he was a Lecturer and then an Associate Professor of Department of Applied Mathematics at Nanjing University of Science and Technology (NUST), Nanjing, China. Since February 1996, he has been an Associate Professor of the Department of Electronic Engineering at NUST. Currently, he is a Postdoctoral Research Fellow in the Center for Computational Electromagnetics, University of Illinois at Urbana-Champaign (UIUC). His current research interests include fast algorithms for computational electromagnetics, scattering and antenna analysis, and ferrite components and their analysis.

Feng Ling (S'97), for a photograph and biography, see p. 1357 of the September 1998 issue of this TRANSACTIONS.

Jian-Ming Jin (S'87–M'89–SM'94), for a photograph and biography, see p. 311 of the March 1998 issue of this TRANSACTIONS.